Journal of Materials Chemistry C

Accepted Manuscript

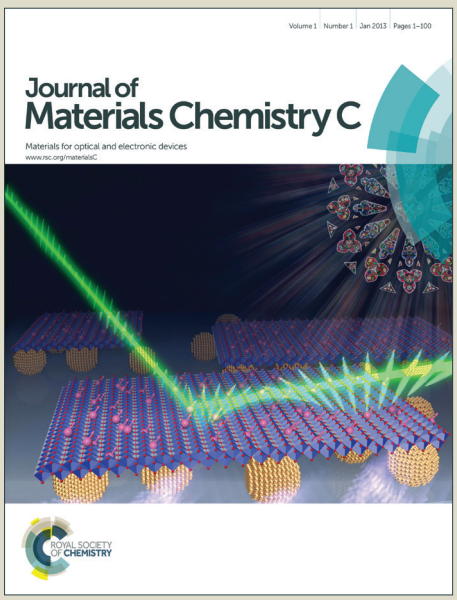

ROYAL SOCIETY OF CHEMISTRY

www.rsc.org/materialsC

Orienting Polydiacetylene Using Aligned Carbon Nanotubes

Xuemei Sun, Xin Lu, Longbin Qiu, Huisheng Peng**

State Key Laboratory of Molecular Engineering of Polymers, Department of Macromolecular Science, and Laboratory of Advanced Materials, Fudan University, Shanghai 200438, China; Email: penghs@fudan.edu.cn, *sunxm@fudan.edu.cn*.

ABSTRACT: The orientation of conjugated polymers is key to enhancing their optical and electronic properties. Here, a general and effective strategy is developed to orient conjugated polymers using aligned carbon nanotubes (CNTs). The application of this strategy is demonstrated using chromatic polydiacetylene (PDA) as a molecular model. Due to the strong interactions between PDA and CNTs, oriented PDA microfibers are produced with the PDA backbones oriented along the direction being perpendicular to the CNT length. The impact of the thickness of the aligned CNTs, the monomer concentration, the degree of polymerization and the heating temperature on the degree of orientation of PDA are carefully studied. A high order parameter of 0.75 is achieved after optimization. The incorporation of aligned CNTs and the orientation of PDA enable a considerably improved chromatic property, i.e., a rapid color change upon heating.

Introduction

The anisotropic structures of organic materials such as conjugated polymers are critically important to the applications of these materials because their intrinsic characteristics, including their optical and electronic properties, originate from the delocalization of π electrons along their backbones.[1] For instance, oriented conjugated polymer chains offer enhanced the charge mobility in field-effect transistors, enable the fabrication of polymer light-emitting diodes that generate polarized light, provide increased energy-conversion efficiency in polymer solar cells and improve the susceptibility of nonlinear optical devices.[2-5] Conjugated polymers have generally been oriented through self-assembly, and such highly ordered structures have been extensively explored on the molecular level.[6] However, ordered structures have been observed only in local regions, and it has not been possible to extend them to the macroscopic scale. Polymer chains can also be oriented through mechanical rubbing, and chains oriented in this manner exhibit anisotropic structures along the rubbing direction, although the orientation is achieved primarily at the rubbed surface.[7,8] In addition, considerable damage is produced during the rubbing process, which significantly decreases the performance of these materials. Therefore, although doing so remains a challenge, it is highly desirable to develop general and effective methods of synthesizing macroscopically oriented conjugated polymer materials with high performance.

Because of their unique structures and remarkable chemical and physical properties, carbon nanotubes (CNTs) have been widely incorporated into conjugated polymers through π-π

interactions. A broad spectrum of conjugated polymers, such as poly (phenylene vinylene) derivatives, poly (3-alkylthiophene) and poly (arylene ethynylene), have been found to interact with CNTs, primarily in dilute solutions.[9-11] Conjugated polymer backbones have been observed to wrap around or extend along the lengths of CNTs, depending on the size and structure of the CNTs and polymers.[12,13] The evaporation of solvents has also been used to produce composite films, although the properties of the resulting films, including their mechanical strength and electrical conductivity, were much lower than expected because of the random dispersion of the CNTs and the non-oriented structure of the polymer backbones. Fortunately, aligned CNT materials have recently been found to effectively orient liquid crystalline polymers through interactions between the CNTs and the side chains of the polymers. Furthermore, an aligned structure of CNTs can further extend the orientation of polymer molecules to the macroscopic scale.[14,15] This phenomenon may shed light on the structural control of conjugated polymers. However, few studies concerning the orientation of conjugated polymers by aligned CNTs have been reported to date.[16]

Polydiacetylene (PDA), which can be easily synthesized using a simple and efficient topochemical polymerization method, represents one of the most explored conjugated polymers because of its unique optical, electronic and sensing properties.[17,18] For instance, PDA had been widely explored for its chromatic transitions, which produce visual color changes under various types of stimulation, including heat, chemicals, light, stress, biomolecules, electric currents and magnetic fields.[18-22] The orientation of the building monomers that polymerize into PDA is key to realizing enhanced sensing and other electronic properties.[5, 23,24]

At the present study, PDA has been oriented by the highly aligned CNT through the interactions between them. PDA appear in microfibers with backbones that are oriented in a direction being perpendicular to the CNT length, and a high degree of orientation with an order parameter of up to 0.75 is achieved. The aligned CNTs also greatly enhanced the thermochromatic properties of the PDA because of the high thermal conductivity of CNTs and the formation of PDA microfibers.

Experimental Section

Materials: Monomers of 10,12-pentacosadiynoic acid ($CH_3(CH_2)_{11}CCCC(CH_2)_8COOH$, >95%), 5,7-eicosadiynoic acid ($CH_3(CH_2)_{11}CCCC(CH_2)_3COOH$, 98.1%) and 5,7-octadecadiynoic acid ($CH_3(CH_2)_9CCCC(CH_2)_3COOH$, 97.4%) were purchased from GFS Chemicals, Inc. (USA). Ethanol was obtained from Shanghai Zhenxing No. 1 Chemical Plant and used as received. Ethylene (99.95%), argon (99.999%) and hydrogen (99.999%) gases were obtained from Shanghai Tomoe Gases Co., Ltd and were used for the synthesis of aligned CNT arrays. Fe and Al_2O_3 were obtained from the Shanghai Institute of Optics and Fine Mechanics and were used for the preparation of the catalysts.

Methods: The monomers were dissolved in ethanol with a concentration higher than 10 mg mL^{-1} (e.g., 15 mg mL^{-1}). After ultrasonic treatment for 10 min, the resulting solutions were filtered using a nylon membrane (pore size of 0.22 μm) and then diluted to 10 mg mL^{-1}. A series of monomer solutions with different concentrations was obtained by either diluting or concentrating the 10 mg

mL^{-1} solution.

Aligned CNT arrays were first synthesized via chemical vapor deposition in a 2-inch-diameter quartz tube furnace. The catalyst was prepared by coating a silicon substrate with Fe (thickness of 1.2 nm) and Al_2O_3 (thickness of 3 nm) through using electron beam evaporation at rates of 0.5 and 2 Å s^{-1}, respectively. Ethylene was used as the carbon source, and a mixture of argon and hydrogen served as the carrier gas. The growth was typically conducted at 740 °C for 10 min with flow rates of 90, 400 and 30 standard cm^3 min^{-1} for ethylene, argon and hydrogen, respectively.

Aligned CNT sheets were dry-drawn from the CNT arrays and stabilized on a glass substrate. Typically, one layer of CNT sheet exhibited an average thickness of ~20 nm, and they could be stacked along the drawing direction to produce thicker sheets. Therefore, the thickness of CNT sheets can be controlled by varying the stacked layer number. An aligned CNT/monomer composite film was prepared by first coating the CNT sheets with the monomer solutions, followed by the evaporation of the solvent and heating at ~65 °C (higher than the melting points of the monomers) for 30 min. The synthesis of the CNT/PDA composite films was then completed through topological polymerization under UV light (wavelength of 254 nm) at room temperature.

Characterization: The structures were characterized via scanning electron microscopy (SEM, Hitachi FE-SEM S-4800, operated at 1 kV) and transmission electron microscopy (TEM, JEOL JEM-2100 F, operated at 200 kV). The thickness of a CNT sheet can be directly measured or

averaged from multilayers of CNT sheets by using a Dektak 150 surface profilometer. Small-angle X-ray scattering (SAXS) patterns were obtained using a Nanostar U SAXS system (Bruker, Germany) equipped with a Cu Kα radiation source. The CNT sheets were attached to the sample holder with the aligned CNTs oriented in the vertical direction. Polarized optical microscopy (POM) was performed using an Olympus BX51 microscope with a rotatable stage. Powder X-ray diffraction (XRD) patterns were obtained using a D8 ADVANCE with DAVINCI.DESIGN diffractometer (Bruker, Germany) equipped with a Cu Kα radiation source operated at 35 kV and 30 mA. UV-Vis, Raman and Fourier transform infrared (FTIR) spectra were recorded using a Shimadzu UV-2550 spectrophotometer, a Renishaw inVia Reflex laser micro-Raman spectrometer with an excitation wavelength of 632.8 nm and a Shimadzu IRPrestige-21 spectrometer, respectively.

Results and Discussion

Aligned CNT sheets were first dry-drawn from CNT arrays that had been previously synthesized via chemical vapor deposition. Figure 1a shows a typical SEM image of one such array with a height of ~280 μm. The CNTs were highly aligned in the array, as observed in a side view at a higher magnification (Figure 1b). Figure 1c presents a TEM image of a spinnable CNT with a multi-walled structure and a diameter of ~12 nm. The as-prepared, single-layer CNT sheets exhibited an average thickness of ~20 nm, and multiple layers of such sheets could be further stacked into thicker sheets along the drawing direction (Figure 1d). If not otherwise specified, a

thickness of ~40 nm was generally utilized. Two-dimensional small-angle X-ray scattering (SAXS) profile with two dense scattering areas in horizontal direction and polarized Raman spectra with Raman intensity in axial direction much larger than radial direction (Figure S1) further indicated the high alignment of the CNT sheets.

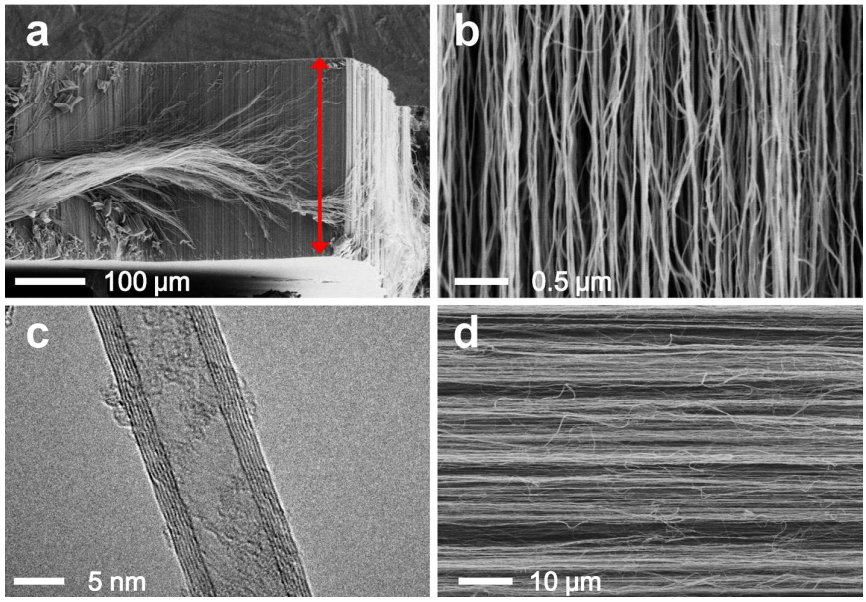

Figure 1. Side-view SEM images of a CNT array at (a) low and (b) high magnifications. (c) High resolution TEM image of a CNT. (d) SEM image of a CNT sheet. The red arrow indicates the height of the CNT array.

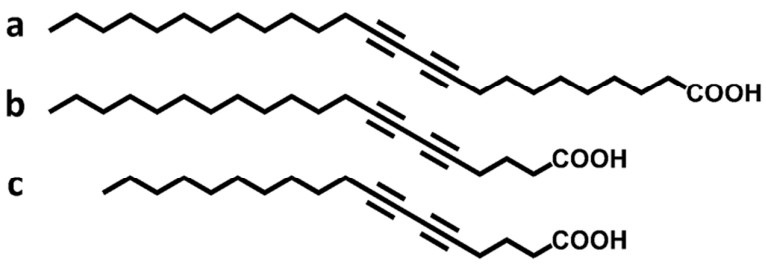

Figure 2. Chemical structures of three diacetylenic monomers: (a) 10,12-pentacosadiynoic acid, (b) 5,7-eicosadiynoic acid and (c) 5,7-octadecadiynoic acid.

The aligned CNT sheets were then coated with the diacetylenic precursors illustrated in Figure 2, followed by the evaporation of the solvent and heating at ~65 °C for 30 min. Here, 10,12-pentacosadiynoic acid (Figure 2a) was mainly investigated. After the samples had cooled to room temperature, microfibers had formed on the surface of aligned CNT sheets and were oriented along the direction perpendicular to the CNT length, as shown in Figure 3a. CNT/PDA composite films were synthesized through the topochemical polymerization of the diacetylenic monomers under UV light, after which the microfiber morphology was well maintained, i.e. uniformly dispersed across the aligned CNT sheets (Figure 3b). By contrast, the PDA formed non-continuous islands rather than microfibers when the diacetylenic monomers were coated onto the glass substrates under the same conditions but without the aid of aligned CNT sheets (Figure S2). Although the monomers were colorless, both the bare PDA and CNT/PDA composite films turned blue (Figure S3).

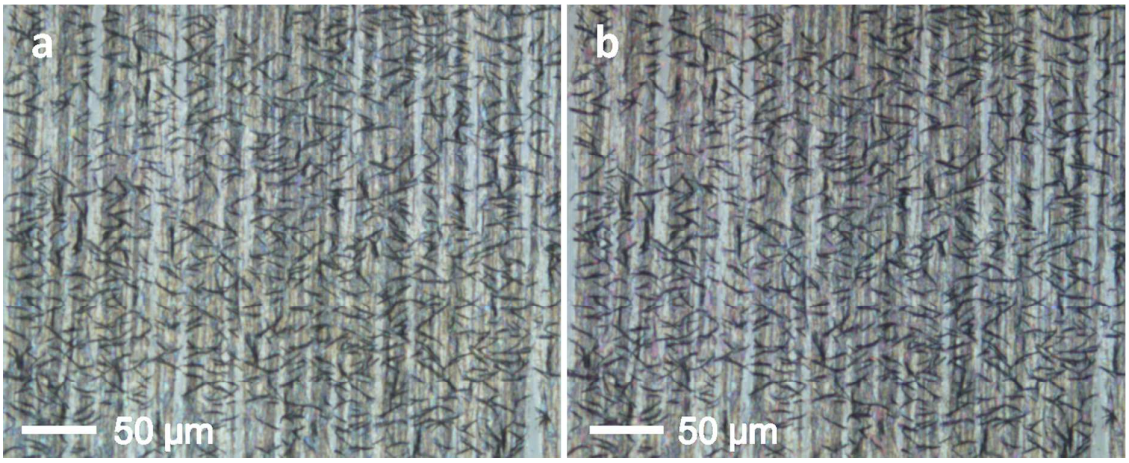

Figure 3. Optical micrographs of a CNT/diacetylenic-monomer composite film (a) before and (b) after polymerization. CNTs were aligned in vertical direction.

Figure 4 presents polarized optical micrographs of the aligned CNT/PDA composite film. The lowest optical transmittance was observed when the CNT length was either parallel or perpendicular to the polarization direction, whereas the highest transmittance was observed at an angle of 45^{o} between the CNT length and either polarization direction. Blue microfibers were clearly observed to be uniformly dispersed on the aligned CNT sheets at a high magnification (Figure S4); these fibers were 15-30 μm long and 0.8-2.0 μm wide. By contrast, no significant differences in the optical transmittances in different directions were detected for the bare PDA films using an orthogonal polarizing microscope (Figure S5). In addition, randomly dispersed PDA microfibers were produced when a networked CNT film was used under the same conditions (Figure S6). Therefore, the aligned structure of the CNTs was responsible for the formation of oriented PDA microfibers.

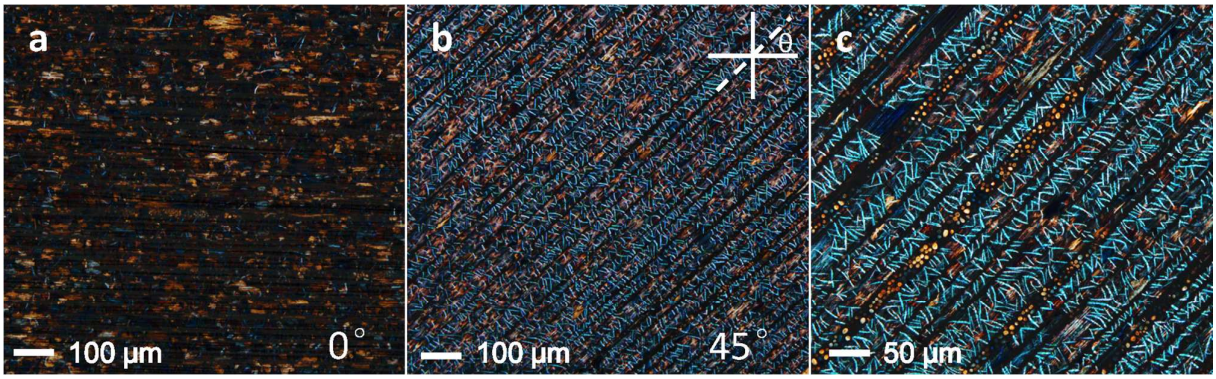

Figure 4. Polarized optical micrographs of a CNT/PDA composite film based on a CNT sheet with a thickness of 40 nm at θ values of (a) 0° and (b, c) 45°. The two solid white lines represent the directions of the optical axes of the two polarizers, whereas the white dashed line represents the direction of CNT alignment.

In order to know the mechanism of the fiber formation, UV-Vis and Raman spectroscopic studies were first performed to gain an understanding of the interactions between the CNTs and PDA. Figure 5a compares the UV-Vis spectra of bare PDA and aligned CNT/PDA composite films. The maximal absorbance of PDA at ~640 nm for the π–π* excitonic band, which is related to the degree of order of the backbone, i.e., the conjugation length, was shifted to a higher wavelength of ~647 nm after the incorporation of the aligned CNTs.[7] Figure 5b compares the Raman spectra of bare CNT, bare PDA and CNT/PDA composite films. The G' band of the CNT sheets was shifted from 2664 to 2657 cm^{-1} in the composite film, and the peaks corresponding to the C≡C and C=C bonds in the PDA were shifted from 2088 to 2073 cm^{-1} and from 1451 to 1445 cm^{-1}, respectively.[25] These results indicated that the aligned CNTs interacted with PDA molecules and increased the effective conjugation lengths of the PDA.

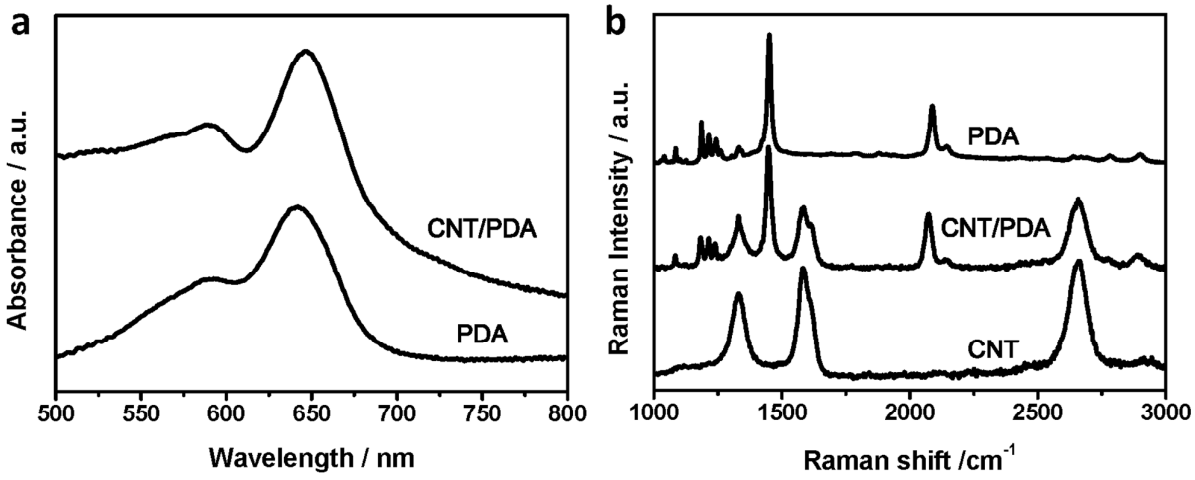

Figure 5. (a) UV-Vis and (b) Raman spectra of bare PDA and aligned CNT/PDA composite films.

The orientation of PDA in the composite film were further measured using both polarized UV-Vis and Raman spectroscopic methods.[7] Figure 6a presents the polarized UV-Vis spectra of the CNT/PDA composite film. When the polarization direction of the light was perpendicular to the CNT length, the composite film exhibited a much higher absorption intensity at the characteristic peak than that was observed for parallel polarization. The UV-Vis absorption spectra were further traced for increasing polarization angles in intervals of 15°. Here, the polarization angle corresponds to the angle between the polarizer and the CNT length. The absorption peak at ~640 nm was recorded to produce the polar plot presented in Figure 6b. The maximal and minimal absorptions were observed at polarization angles of 90°/270° and 0°/180°, respectively. By contrast, a constant absorption intensity as a function of the polarization angle was observed for the bare PDA film (Figure S7a).

The Raman spectra were also recorded to determine the orientation of the PDA (Figure 6c).[26] As previously mentioned, aligned CNTs exhibited much higher intensity in the parallel direction than in perpendicular direction to the CNT length (Figure S1b). While In CNT/PDA composite film, the vibrational stretching modes for both triple (2073 cm^{-1}) and double (1445 cm^{-1}) carbon bonds of PDA were much higher in intensity in the perpendicular direction than in the parallel direction relative to the CNT length. When measured at a local area, the polarized Raman spectra of a single PDA microfiber in the composite film could be obtained with the intensity along the axial direction being much higher than that along the radial direction of the PDA microfiber, which agrees with the dichroic ratio of the composite film (Figure S8). Similarly, the Raman intensities of the bare PDA were independent of the polarization direction (Figure S7b). In both UV-Vis and Raman spectra, the higher intensity observed in the perpendicular direction was ascribed to the preferred orientation of the PDA backbones in the direction being perpendicular to the CNT length, as shown in Figure 6d. In other words, the PDA backbones were oriented along the microfiber axis.

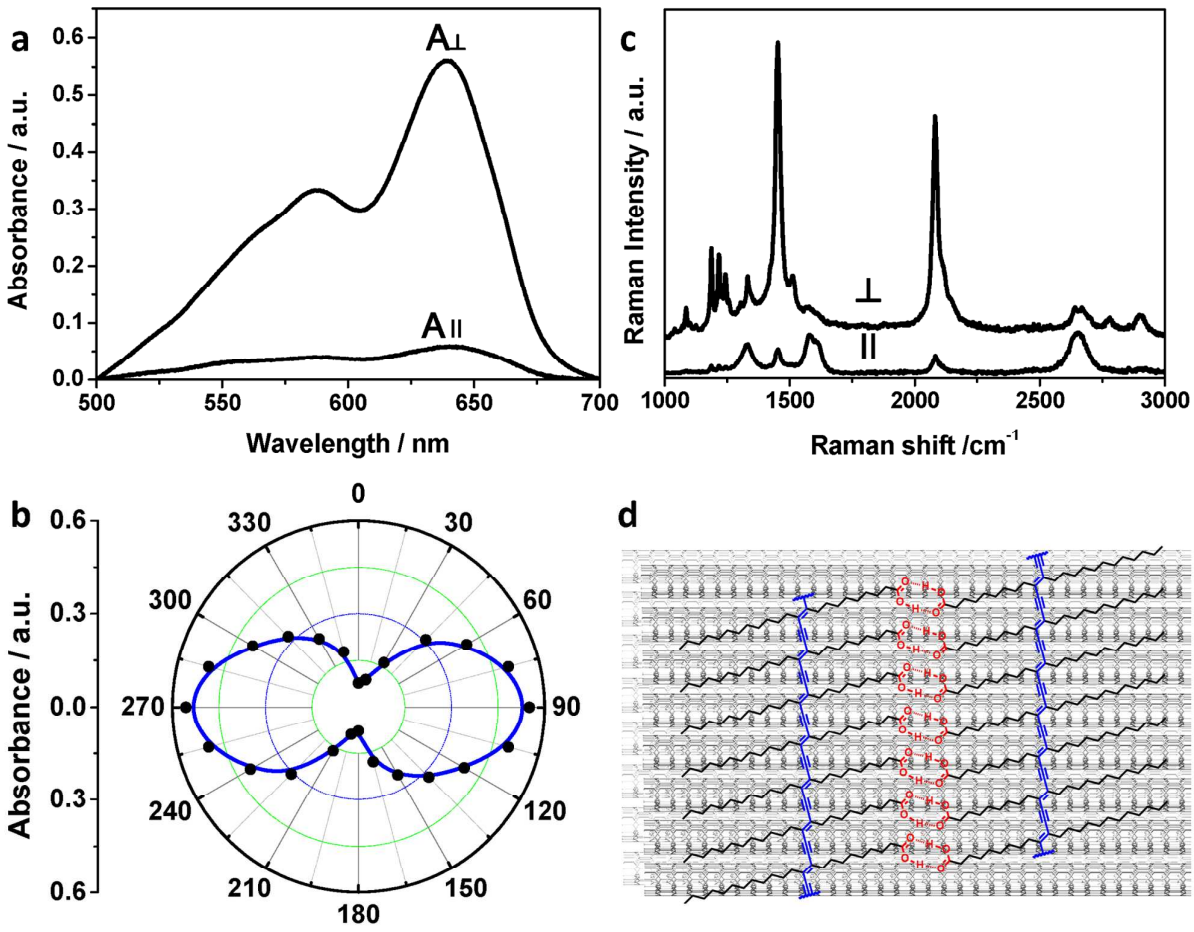

Figure 6. (a) Polarized UV−Vis absorption spectra of the CNT/PDA composite film. $A_{//}$ and $A_{\perp}$ correspond to the absorbances in the directions parallel and perpendicular to the CNT length, respectively. (b) Angle-dependent UV−Vis absorbance at ~640 nm. (c) Polarized Raman spectra of the CNT/PDA composite film. (d) Schematic illustration to the PDA orientation being perpendicular to the CNT length.

It has been previously reported that diacetylenic monomers will stack into a bi-layered structure because the carboxyl groups are inclined to produce dimers.[27,28] After polymerization, the resultant PDA will form a bimolecular lamellar structure with the backbones perpendicular to the

layer-stacking direction.[29] Infrared spectroscopy was used to investigate the differences in the carboxyl groups of the bare PDA film and the aligned CNT/PDA composite film (Figure S9). The characteristic C=O stretching peak was observed at ~1695 cm^{-1} for both films, indicating the formation of dimers through hydrogen bonding in the carboxylic acid head group.[30] It has been also well established that diacetylenic monomers must be highly ordered to react with each other to produce PDA as desired and that the polymerization process does not change the molecular organization.[31] Therefore, the stacking directions of the monomers determine the orientations of the PDA backbones. When the monomers are stacked along the same direction, the resultant PDA will be oriented accordingly. Fiber-shaped aggregates did indeed form upon the coating of the aligned CNT sheets with the monomer solutions (Figure 3), and similar X-ray diffraction patterns were observed before and after polymerization (Figure S10). Therefore, the monomer molecules are inclined to extend along the CNT length, similar to the azobenzene-containing liquid crystal mesogens,[14,15] and stack perpendicularly due to π–π interactions, although the other non-covalent interactions such as hydrogen bonding, hydrophobic interactions and van der Waals forces may also make contributions.[31] The stacked diacetylenic monomers are further assembled into microfibers oriented in the direction being perpendicular to the CNT length. After polymerization, the PDA backbone lay along the monomer-stacking direction, i.e., parallel to the microfiber axis and perpendicular to the CNT length.

The degree of orientation of the PDA was calculated using either the dichroic ratio (R) or the order parameter (S).[32] The dichroic ratio was obtained as follows: $R = A_{\perp}/A_{//}$ or $I_{\perp}/I_{//}$, where $A_{//}$ and $A_{\perp}$

correspond to the absorbance intensities in the UV-Vis spectra with the incident light polarized parallel or perpendicular to the CNT length, respectively, and $I_{//}$ and $I_{\perp}$ correspond to the Raman intensities with the incident light polarized parallel or perpendicular to the CNT length, respectively. The dichroic ratio reached ~10, according to both UV-Vis and Raman spectra. And the orientation of the PDA could also be described using the two-dimensional order parameter (S), defined as $S=(R-1)/(R+2)$,[32] which reached a high value of 0.75.

The orientation of conjugated polymer can be also achieved by using the rubbed polymer substrate such as polyimide, and the conjugated backbones have been reported to be oriented along the rubbing direction. Here PDA was deposited on the mechanically rubbed polyimide film for the orientation study (Figure S11). PDA exhibited a higher absorption intensity at the characteristic peak in the perpendicular direction than that along the parallel direction relative to the rubbing direction. Therefore, the aligned CNTs generated a similar orientation effect to the rubbed polymer substrate but with much higher orientation degrees.

The impact of the CNT-sheet thickness, the concentration of the monomer solution, the degree of polymerization and the heating temperature on the PDA microfibers was also carefully studied (Figure 7). The density of the PDA microfibers gradually increased with increasing CNT-sheet thickness. By contrast, the average order parameters of the composite films derived from CNT sheets with thicknesses of 20 and 40 nm were similar, and the order parameter gradually decreased as the thickness increased further, e.g., ~0.60 at 120 nm (Figure 7a). This phenomenon may be

explained in terms of variations in the interaction between the CNTs and the PDA. The voids among the aligned CNTs decreased with increasing thickness, thus allowing for more CNTs to interact with the diacetylenic precursors on the surface, which favored the growth of more PDA microfibers. However, the increased PDA microfibers tended to aggregate with each other during the growth, causing them to less effectively interact with the aligned CNTs, thus leading the orientation to decrease as the CNT-sheet thickness increased further (Figure S12). Similarly, there was also an optimal monomer concentration of ~10 mg mL^{-1} to obtain the maximal order parameter (Figure 7b). It is worth noting that smaller and fewer PDA microfibers were produced at lower concentrations, whereas larger and more abundant microfibers were obtained at higher concentrations (Figure S13). Interestingly, the order parameters increased during polymerization, which may have induced the re-organization of the alkyl side chains to form more ordered structures (Figure 7c).

The heat treatment was found to significantly increase the order parameter. For the as-prepared CNT/PDA composite films and those prepared by heating at low temperatures (below the melting point of the monomer), a low order parameter of ~0.32 was obtained, which was much lower than the order parameter of 0.7 that was obtained for the composite film that was prepared by heating at temperatures above the melting point of the monomer (Figure 7d). They showed micro-flake structure rather than microfibers (Figure S14). In other words, the heat treatment induced closer stacking of the monomers along the CNT length because of the higher freedom of the interaction between the PDA and the CNTs. No significant differences in the order parameter were observed for heating at different temperatures above the melting point.

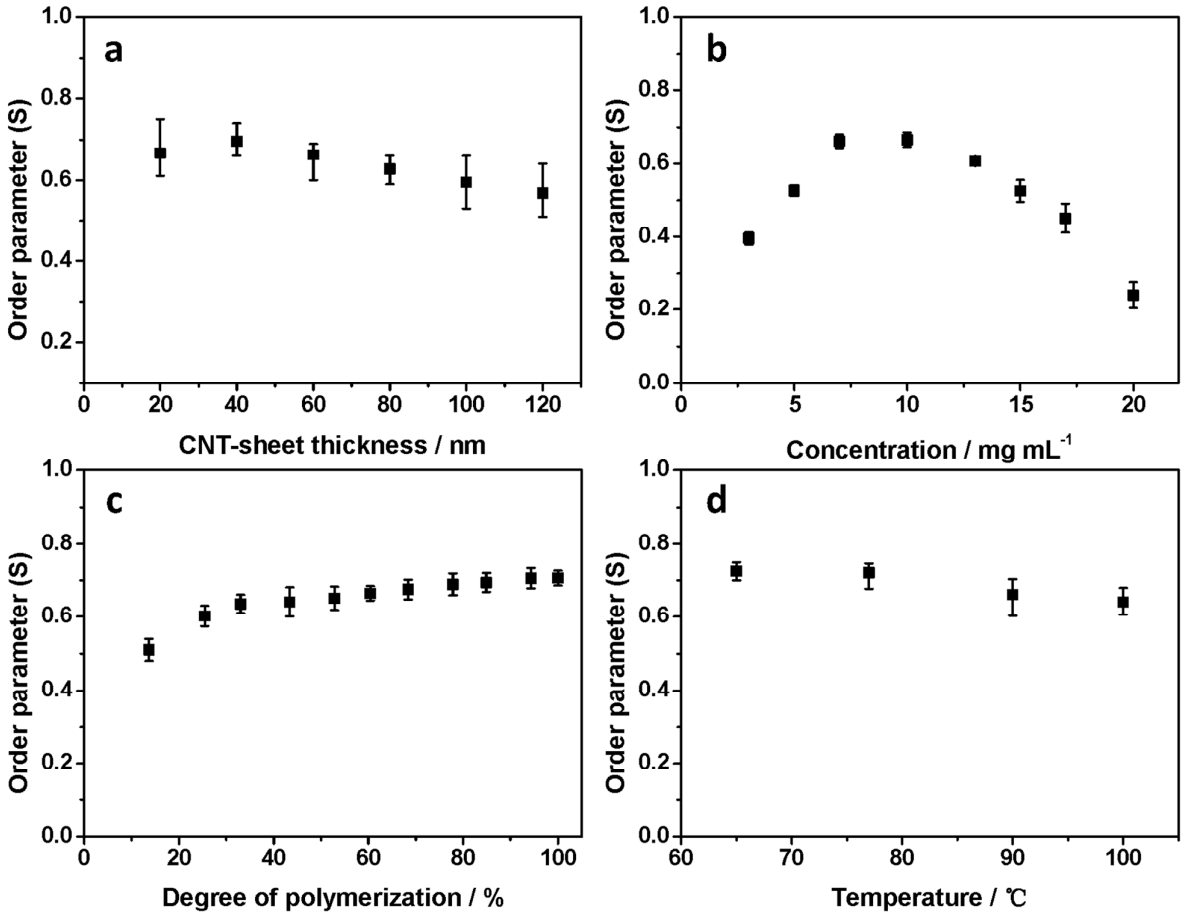

Figure 7. Dependence of the degree of orientation on (a) the CNT-sheet thickness, (b) the concentration of the monomer solution, (c) the degree of polymerization of the PDA, and (d) the temperature of the heat treatment.

To investigate the generality of orientation using aligned CNT sheets, another two monomers (Figures 2b and 2c), 5,7-octadecadiynoic acid and 5,7-eicosadiynoic acid, were also used in place of 10,12-pentacosadiynoic acid. The resulting PDA backbones were also oriented in the direction perpendicular to the CNT length according to the polarized UV-Vis spectra (Figure S15 and Table

S1). Therefore, this method may be widely used to synthesize various aligned PDA materials with controlled side chains by varying the monomer structure. In addition, the aligned CNT sheets can also induce the orientation of other conjugated polymers such as polythiophene and polyfluorene (Figure S16). However, both of them formed continuous films rather than fibers like PDA, and the polymer backbones are parallel to the CNT length with order parameters of 0.34 and 0.32, respectively. More efforts are required to understand the different morphologies between PDA and polythiophene and polyfluorene on the aligned CNT sheet.

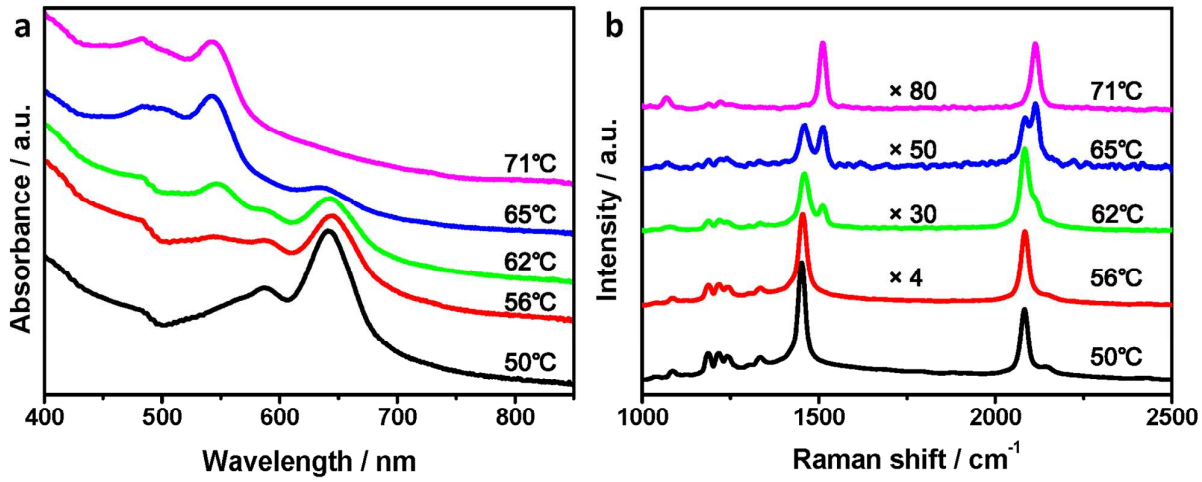

Figure 8. (a) UV−Vis absorption spectra and (b) Raman spectra of the aligned CNT/PDA composite film after being heated to various temperatures.

PDA has been widely demonstrated to exhibit a chromatic transition, typically from blue to red, in response to heating because of the reduction of its effective conjugation length.[17] In this study, the thermochromatic properties of the CNT/PDA composite films were investigated. UV-Vis and

Raman spectroscopy was used to confirm the structural change during the thermochromatic transition (Figure 8). In the UV-Vis spectra, the intensity of the peak at ~640 nm for the blue phase gradually decreased with increasing temperature, whereas the intensity of the peak at ~540 nm for the red phase correspondingly increased. In the Raman spectra, the two characteristic peaks at 2073 and 1445 cm^{-1} (triple and double carbon bonds, respectively) for the blue phase decreased in intensity during the heating process, and replaced by two characteristic peaks at 2114 and 1511 cm^{-1} for the red phase gradually.[33] Both spectra therefore indicated a chromatic transition from blue to red. Figures S17 and S18 present the UV-Vis spectra of bare PDA and randomly dispersed CNT/PDA composite films, respectively, which share a similar behavior but exhibit color changes at different temperatures. The blue peak of the bare PDA film disappeared at ~85 °C, which was a higher temperature than those at which the blue peaks were observed to disappear for the randomly dispersed and aligned CNT/PDA composites (71-77 °C).

To evaluate the rate of the chromatic transition, the colorimetric response (*CR*) was calculated using the following equation: $CR=[(B_0-B_T)/B_0]\times100\%$, where $B=A_{blue}/(A_{blue}+A_{red})$. [34] Here, A_{blue} and A_{red} represent the absorbance intensities of the blue (~640 nm) and red (~540 nm) phases in the UV-Vis spectrum, respectively, and B_0 and B_T correspond to the cases before and after heating, respectively. Both the bare PDA and CNT/PDA composite films were heated from 40 to 90 °C at a rate of 5 °C min^{-1}. Figure 9 presents a comparison among the bare PDA, the randomly dispersed CNT/PDA composite and several aligned CNT/PDA composites with various PDA order parameters. The bare PDA exhibited a color change within 510 s. The introduction of CNTs caused the randomly

dispersed CNT/PDA composite to complete its thermochromatic transition within 480 s. The rate of the chromatic transition was further improved in the aligned CNT/PDA composites and exhibited greater enhancement as the order parameter increased, i.e., the transition proceeded within 450, 420 and 405 s at order parameters of 0.32, 0.53 and 0.70, respectively. Interestingly, the critical temperatures at which the color change began increased from the bare PDA to the randomly dispersed CNT/PDA and, finally, to the aligned CNT/PDA composites in increasing order of the order parameters.

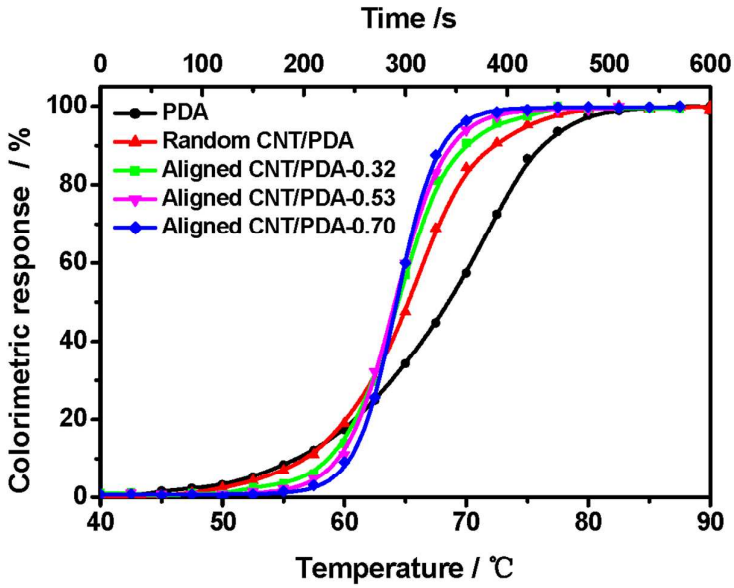

Figure 9. Colorimetric responses of bare PDA, randomly dispersed CNT/PDA and aligned CNT/PDA composites as a function of temperature at a heating rate of 5 °C min^{-1}. The order parameters of PDA in the aligned CNT/PDA composites were 0.32, 0.53 and 0.7.

The phenomena described above may be explained in terms of the different microstructures of the

composites. On the one hand, CNTs serve as robust frameworks to stabilize PDA moieties with higher transition temperatures, and higher alignment of the CNTs increases their stability.[24] On the other hand, thermally conductive CNTs also function as effective pathways for heat transport. For instance, it requires less time for a CNT/PDA composite to initiate a color change under heating at the same temperature of 65 °C compared to the bare PDA (Figure S19). A more aligned structure further increases the transport efficiency, leading to a more rapid chromatic transition.[35] In addition, the smaller size of the uniform PDA microfibers in the CNT/PDA composite compared with the aggregates in the bare PDA likely contributes to a rapid and sharp thermochromatic transition.[36] The rapid color change under heating endowed the aligned CNT/PDA composite with various sensing applications such as a detector to reflecting the temperature change in environment. As a demonstration, a blue composite film was pasted onto a cup as a warning label. It remained blue at a temperature below 70 °C and immediately became red beyond this point (Figure S20). Therefore, it is convenient to determine whether the liquid inside is safe for drinking or not.

Conclusion

A general and effective method has been developed for the synthesis of macroscopically oriented PDA by aligned CNT sheets. These PDA formed into microfibers with conjugated backbones perpendicularly oriented relative to the lengths of the aligned CNTs. The degree of orientation of the PDA was found to depend on the thickness of the CNT sheet, the monomer concentration, the degree of polymerization and the heating temperature, and a high order parameter of 0.75 was

achieved. The rate of the chromatic transition in the PDA was also greatly increased through the introduction of aligned CNTs, which induced the formation of microfibers and exhibited high thermal conductivity.

Supporting Information

Electronic Supplementary Information (ESI) is available.

Acknowledgements

This work was supported by MOST (2011CB932503), NSFC (21225417, 51403038), STCSM (12nm0503200), China Postdoctoral Science Foundation (2047M560290), the Fok Ying Tong Education Foundation, the Program for Special Appointments of Professors at Shanghai Institutions of Higher Learning, and the Program for Outstanding Young Scholars of the Organization Department of the CPC Central Committee.

Notes and references

1. T.-Q. Nguyen, J. Wu, V. Doan, B. J. Schwartz and S. H. Tolbert, *Science*, 2000, **288**, 652-656.
2. H. Sirringhaus, R. J. Wilson, R. H. Friend, M. Inbasekaran, W. Wu, E. P. Woo, M. Grell and D. D. C. Bradley, *Appl. Phys. Lett.*, 2000, **77**, 406-408.
3. M. Grell, W. Knoll, D. Lupo, A. Meisel, T. Miteva, D. Neher, H.-G. Nothofer, U. Scherf and A.

Yasuda, *Adv. Mater.*, 1999, **11**, 671-675.

4. J. S. Kim, Y. Park, D. Y. Lee, J. H. Lee, J. H. Park, J. K. Kim and K. Cho, *Adv. Funct. Mater.*, 2010, **20**, 540-545.
5. T. Kanetake, K. Ishikawa, T. Hasegawa, T. Koda, K. Takeda, M. Hasegawa, K. Kubodera and H. Kobayashi, *Appl. Phys. Lett.*, 1989, **54**, 2287-2289.
6. Y. Kubo, Y. Kitada, R. Wakabayashi, T. Kishida, M. Ayabe, K. Kaneko, M. Takeuchi and S. Shinkai, *Angew. Chem. Int. Ed.*, 2006, **45**, 1548-1553.
7. I. Moggio, J. Le Moigne, E. Arias-Marin, D. Issautier, A. Thierry, D. Comoretto, G. Dellepiane and C. Cuniberti, *Macromolecules*, 2001, **34**, 7091-7099.
8. L. Hartmann, K. Tremel, S. Uttiya, E. Crossland, S. Ludwigs, N. Kayunkid, C. Vergnat and M. Brinkmann, *Adv. Funct. Mater.*, 2011, **21**, 4047-4057.
9. J. Chen, H. Liu, W. A. Weimer, M. D. Halls, D. H. Waldeck and G. C. Walker, *J. Am. Chem. Soc.*, 2002, **124**, 9034-9035.
10. J. Zou, L. Liu, H. Chen, S. I. Khondaker, R. D. McCullough, Q. Huo and L. Zhai, *Adv. Mater.*, 2008, **20**, 2055-2060.
11. D. W. Steuerman, A. Star, R. Narizzano, H. Choi, R. S. Ries, C. Nicolini, J. F. Stoddart and J. R. Heath, *J. Phys. Chem. B*, 2002, **106**, 3124-3130.
12. A. Star, J. F. Stoddart, D. Steuerman, M. Diehl, A. Boukai, E. W. Wong, X. Yang, S.-W. Chung, H. Choi and J. R. Heath, *Angew. Chem. Int. Ed.*, 2001, **40**, 1721-1725.
13. H. W. Lee, Y. Yoon, S. Park, J. H. Oh, S. Hong, L. S. Liyanage, H. Wang, S. Morishita, N. Patil, Y. J. Park, J. J. Park, A. Spakowitz, G. Galli, F. Gygi, P. H. S. Wong, J. B. H. Tok, J. M. Kim

and Z. Bao, *Nat. Commun.*, 2011, **2**, 541.

14. W. Wang, X. Sun, W. Wu, H. Peng and Y. Yu, *Angew. Chem. Int. Ed.*, 2012, **51**, 4644-4647.
15. X. Sun, W. Wang, L. Qiu, W. Guo, Y. Yu and H. Peng, *Angew. Chem. Int. Ed.*, 2012, **51**, 8520-8524.
16. X. Lu, Z. Zhang, H. Li, X. Sun and H. Peng, *J. Mater. Chem. A*, 2014, **2**, 17272-17280.
17. X. Sun, T. Chen, S. Huang, L. Li and H. Peng, *Chem. Soc. Rev.*, 2010, **39**, 4244-4257.
18. B. Yoon, S. Lee and J.-M. Kim, *Chem. Soc. Rev.*, 2009, **38**, 1958-1968.
19. H. Peng, X. Sun, F. Cai, X. Chen, Y. Zhu, G. Liao, D. Chen, Q. Li, Y. Lu, Y. Zhu and Q. Jia, *Nat. Nanotechnol.*, 2009, **4**, 738-741.
20. X. Chen, L. Li, X. Sun, Y. Liu, B. Luo, C. Wang, Y. Bao, H. Xu and H. Peng, *Angew. Chem. Int. Ed.*, 2011, **50**, 5486-5489.
21. X. Sun, T. Chen, S. Huang, F. Cai, X. Chen, Z. Yang, L. Li, H. Cao, Y. Lu and H. Peng, *J. Phys. Chem. B*, 2010, **114**, 2379-2382.
22. G. Zou, H. Jiang, Q. Zhang, H. Kohn, T. Manaka and M. Iwamoto, *J. Mater. Chem.*, 2010, **20**, 285-291.
23. Y. Lu, Y. Yang, A. Sellinger, M. Lu, J. Huang, H. Fan, R. Haddad, G. Lopez, A. R. Burns, D. Y. Sasaki, J. Shelnutt and C. J. Brinker, *Nature*, 2001, **410**, 913-917.
24. H. Peng, J. Tang, L. Yang, J. Pang, H. S. Ashbaugh, C. J. Brinker, Z. Yang and Y. Lu, *J. Am. Chem. Soc.*, 2006, **128**, 5304-5305.
25. R. H. Baughman, J. D. Witt and K. C. Yee, *J. Chem. Phys.*, 1974, **60**, 4755-4759.
26. Z. Iqbal, R. R. Chance and R. H. Baughman, *J. Chem. Phys.*, 1977, **66**, 5520-5525.

27. T. Shimogaki and A. Matsumoto, *Macromolecules*, 2011, **44**, 3323-3327.

28. S. R. Diegelmann and J. D. Tovar, *Macromol. Rapid. Comm.*, 2013, **34**, 1343-1350.

29. V. Enkelmann, in *Polydiacetylenes*, Ed: H.-J. Cantow, Springer Berlin Heidelberg, 1984, pp. 91-136.

30. A. Lio, A. Reichert, D. J. Ahn, J. O. Nagy, M. Salmeron and D. H. Charych, *Langmuir*, 1997, **13**, 6524-6532.

31. W. Zhou, Y. Li and D. Zhu, *Chem. Asian. J.*, 2007, **2**, 222-229.

32. D. L. Thomsen, P. Keller, J. Naciri, R. Pink, H. Jeon, D. Shenoy and B. R. Ratna, *Macromolecules*, 2001, **34**, 5868-5875.

33. L. Yu and S. L. Hsu, *Macromolecules*, 2012, **45**, 420-429.

34. A. Reichert, J. O. Nagy, W. Spevak and D. Charych, *J. Am. Chem. Soc.*, 1995, **117**, 829-830.

35. A. M. Marconnet, N. Yamamoto, M. A. Panzer, B. L. Wardle and K. E. Goodson, *ACS Nano*, 2011, **5**, 4818-4825.

36. A. Potisatityuenyong, R. Rojanathanes, G. Tumcharern and M. Sukwattanasinitt, *Langmuir*, 2008, **24**, 4461-4463.

Table of Contents

A general and effective strategy is developed to orient conjugated polymers, such as polydiacetylene, using aligned carbon nanotubes.